

**OPEN ACCESS**

## Ultra-Small Fe<sub>2</sub>N/N-CNTs as Efficient Bifunctional Catalysts for Rechargeable Zn-Air Batteries

To cite this article: Ningning Zhang *et al* 2020 *J. Electrochem. Soc.* **167** 020505

View the [article online](#) for updates and enhancements.

### You may also like

- [Nitrogen-Doped Carbon Nanotubes Encapsulated Cobalt Nanoparticles Hybrids for Highly Efficient Catalysis of Oxygen Reduction Reaction](#)  
Xiaohan Wang, Feifei Zhang, Yang Liu et al.
- [Amperometric Response Characteristics of Rabeprazole at N-Doped CNTs-Chitosan Nanosensor in Solubilized System](#)  
Dhanjai and Ankita Sinha
- [Investigation of Transition Metal-Based \(Mn, Co, Ni, Fe\) Trimetallic Oxide Nanoparticles on N-doped Carbon Nanotubes as Bifunctional Catalysts for Zn-Air Batteries](#)  
Drew Aasen, Michael P. Clark and Douglas G. Ivey



### Your Lab in a Box!

The PAT-Tester-i-16: All you need for Battery Material Testing.

- ✓ All-in-One Solution with integrated Temperature Chamber!
- ✓ Cableless Connection for Battery Test Cells!
- ✓ Fully featured Multichannel Potentiostat / Galvanostat / EIS!

[www.el-cell.com](http://www.el-cell.com) +49 40 79012-734 [sales@el-cell.com](mailto:sales@el-cell.com)

**EL-CELL**<sup>®</sup>  
electrochemical test equipment





# Ultra-Small Fe<sub>2</sub>N/N-CNTs as Efficient Bifunctional Catalysts for Rechargeable Zn-Air Batteries

Ningning Zhang,<sup>1,2</sup> Shilei Xie,<sup>1,z</sup> Wenlong Wang,<sup>1</sup> Dong Xie,<sup>1</sup> Deliang Zhu,<sup>2</sup> and Faliang Cheng<sup>1,z</sup>

<sup>1</sup>Guangdong Engineering and Technology Research Centre for Advanced Nanomaterials, School of Environment and Civil Engineering, Dongguan University of Technology, Dongguan 523808, People's Republic of China

<sup>2</sup>Guangdong Research Center for Interfacial Engineering of Functional Materials, Shenzhen Key Laboratory of Special Functional Materials, College of Materials Science and Engineering, Shenzhen University, Shenzhen 518060, People's Republic of China

Zinc-air batteries (ZABs) have been considered as promising next-generation batteries due to their natural abundance, flat discharge voltage and high theoretical specific energy density. However, the wide application of these ZABs is seriously hindered by the high cost and poor electrochemical stability of noble electrocatalysts. In this paper, we develop a facile method to prepare ultra-small iron-based nitride and nitrogen doped carbon nanotubes (Fe<sub>2</sub>N/N-CNTs) hybrid materials as bifunctional electrocatalysts for ZABs. In the presence of CNTs with large surface areas, ultra-small Fe<sub>2</sub>N nanoparticles with the diameter of around 5 nm are successfully prepared. The oxygen reduction reaction (ORR) activity of Fe<sub>2</sub>N/N-CNTs is comparable to the Pt/C, while the oxygen evolution reaction (OER) activity is much better than the Pt/C. At last, the home-made ZABs with Fe<sub>2</sub>N/N-CNTs have significant rechargeable activities and cyclic stability.

© 2020 The Author(s). Published on behalf of The Electrochemical Society by IOP Publishing Limited. This is an open access article distributed under the terms of the Creative Commons Attribution 4.0 License (CC BY, <http://creativecommons.org/licenses/by/4.0/>), which permits unrestricted reuse of the work in any medium, provided the original work is properly cited. [DOI: 10.1149/1945-7111/ab6317]



Manuscript submitted September 9, 2019; revised manuscript received November 12, 2019. Published January 7, 2020.

As one of efficient energy storage devices, metal-air battery is made to deal with the question of renewable resources, such as solar and wind, which can't offer steady output voltage and current.<sup>1-4</sup> Zinc-air battery (ZAB), as one of the most promising metal-air batteries, has drawn increasing attention due to its unique propriety of low cost, low toxicity, flat discharge voltage and high theoretical specific energy density (1084 Wh kg<sup>-1</sup>).<sup>5-7</sup> Up to now, Pt-based<sup>8,9</sup> and Ru-based 9 materials are widely used for air electrode in ZABs, since they have remarkable electrocatalytic performance to OER or ORR. However, these catalysts suffered from high cost and poor electrochemical stability, which hindered their application in modern society.<sup>10-13</sup> Therefore, it is highly expected to develop bifunctional electrocatalysts with low-cost, superior activity and stability.

Recently, electrocatalysts containing transition metal elements, such as nickel,<sup>5,14,15</sup> iron,<sup>16,17</sup> cobalt,<sup>18-21</sup> and manganese,<sup>22</sup> were studied as potential candidates for OER and ORR. Among these candidates, iron-based catalysts have been attracted great attention due to distinct electronic structures, low cost and high stability.<sup>23</sup> For example, Qiao et al.<sup>24</sup> developed a new method to prepare 3D Fe-PANI-hydrogel catalyst by annealing the precursors at 900 °C under Ar atmosphere. The 3D Fe-PANI-hydrogel catalyst showed higher ORR activity with an onset potential of 0.95 V vs RHE. Xiao et al.<sup>25</sup> synthesized Fe<sub>2</sub>N nanocrystal and incorporated them into mesoporous nitrogen-doped graphitic carbon spheres (Fe<sub>2</sub>N/MNGCS) by annealed the precursors of FeCl<sub>3</sub> and PDA at 700 °C and 750 °C, respectively. The Fe<sub>2</sub>N/MNGCS showed comparable ORR activity to that of commercial Pt/C catalyst in alkaline media. However, these methods always suffered with complicated preparation process, uncontrollable generation of iron oxides with poor activity, and agglomeration of nanoparticles (NPs) due to the high annealed temperature. Consequently, it is highly desirable to find an effective and commercial way to prepare durable and cost-effective electrocatalysts for efficient ZABs.

In this work, we developed a facile method to prepare ultra-small Fe<sub>2</sub>N/N-CNTs hybrid materials for ORR and ZABs, at a relative lower temperature of 600 °C in NH<sub>3</sub> atmosphere compared to recent

literatures.<sup>24,25</sup> The CNTs here not only provided large surface areas for the reaction and growth of Fe<sub>2</sub>N, but also restricted the aggregation of NPs during preparing process. The as-prepared Fe<sub>2</sub>N NPs in Fe<sub>2</sub>N/N-CNTs was around 5 nm, which is much smaller than the pure Fe<sub>2</sub>N NPs. As a result, thus Fe<sub>2</sub>N/N-CNTs showed outstanding and efficient activity and durability for ORR and OER, with small reversible oxygen overpotential of around 0.89 V, which showed promising prospect for metal-air batteries. In addition, home-made ZABs with Fe<sub>2</sub>N/N-CNTs as air cathode also deliver outstanding long-term stability. It is believed that this work may bring new method for the synthesis of ultra-small electrocatalysts with low cost and long durability for rechargeable ZABs.

## Experimental

FeOOH/CNTs were synthesized based on previous reports with minor modifications.<sup>26</sup> Firstly, 0.27 g FeCl<sub>3</sub> 6H<sub>2</sub>O and 0.54 g CNTs were added to 80 ml C<sub>2</sub>H<sub>5</sub>OH. Then, 0.24 g of NH<sub>4</sub>HCO<sub>3</sub> was added to the above solution and stirred at room temperature for 8 h. Lately, the mixture was washed several times and dried by freeze-drying for 12 h. Finally, the FeOOH/CNTs calcined at 600 °C for 3 h in NH<sub>3</sub> atmosphere with a ramp rate of 5 °C per min. In comparison, Fe<sub>2</sub>N NPs were also prepared by calcined FeOOH NPs at the same situation as FeOOH/CNTs.

Scanning electron microscope (SEM) images were taken with a JSM-6701F (JEOL) with 20 kV accelerating voltage. Transmission electron microscope (TEM) images were acquired with JEM2010-HR. Powder X-ray diffraction (XRD) patterns were collected on a Rigaku Ultima-IV diffractometer instrument with Cu K $\alpha$  radiation. X-ray photoelectron spectroscopy (XPS) was performed using a Thermo Scientific K-alpha spectrometer with chromatized Al K $\alpha$  radiation.

All electrochemical measurements were performed with CHI 760E electrochemical workstation and modulated speed electrode rotator (PINE, Durham). The samples on glassy carbon electrode was working electrode, while Pt plate was counter electrode and Hg/HgO electrode was reference electrode. For long-term test, a carbon electrode was adopted as the counter electrode to exclude possibility of platinum dissolution form the counter electrode. The reference potential measured with Hg/HgO was converted into reversible hydrogen electrode (RHE) by following

<sup>z</sup>E-mail: xieshil@dgut.edu.cn; chengfl@dgut.edu.cn

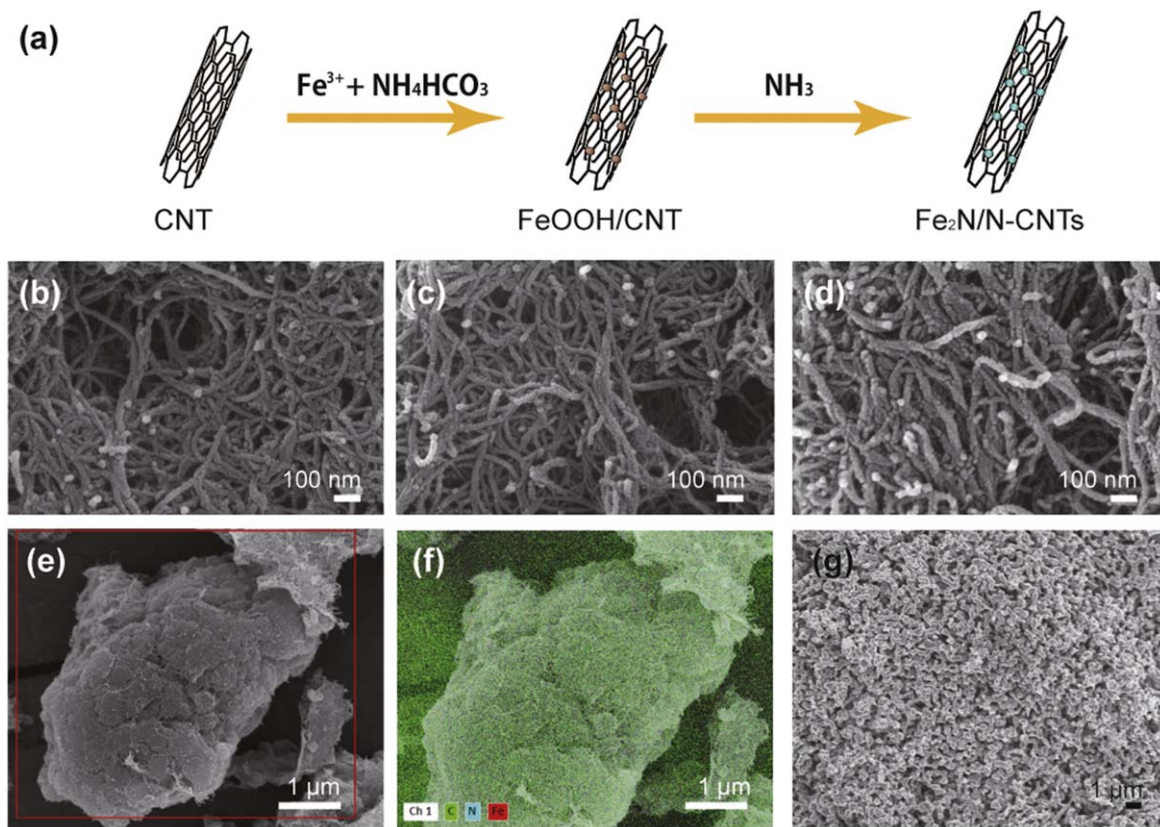


**Figure 1.** (a) Schematic illustration of the fabrication process of Fe<sub>2</sub>N/N-CNTs hybrid materials. SEM images of (b) CNTs, (c) FeOOH/CNTs, (d) and (e) Fe<sub>2</sub>N/N-CNTs. (f) EDS mapping image Fe, N and C for Fe<sub>2</sub>N/N-CNTs. (e) SEM image of Fe<sub>2</sub>N.

formula:

$$E_{RHE} = E_{Hg/HgO} + 0.098 \text{ V} + 0.059 \text{ pH} \quad [1]$$

The catalyst ink was prepared with 2.0 mg of catalyst, 1 ml isopropanol, 0.05 ml of 5 wt.% Nafion (Sigma-Aldrich), and 1 ml water after sonication for 1 h. The working electrode was prepared by dropping 20 μl of catalyst ink on a polished glassy carbon electrode.

Rotating ring-disk electrode (RRDE) measurement was performed to determine the total electron transfer number ( $n$ ) and HO<sub>2</sub><sup>-</sup> yield percent (HO<sub>2</sub><sup>-</sup>%) by following formulas:

$$n = \frac{4N \cdot I_{disk}}{I_{ring} + N \cdot I_{disk}} \quad [2]$$

$$HO_2^{-}\% = \frac{200I_{ring}}{I_{ring} + N \cdot I_{disk}} \quad [3]$$

where  $I_{disk}$  and  $I_{ring}$  are the collected currents at the disk and ring electrode, respectively.  $N$  is RRDE collection efficiency, which was determined to be 0.37.

The ZAB was assembled with samples loaded on clean nickel foam as air-cathode, polished Zn plate as anode, and aqueous solution containing 6 M KOH and 0.2 M Zn(CH<sub>3</sub>COO)<sub>2</sub> as electrolyte, respectively. Fe<sub>2</sub>N/N-CNTs, acetylene black and Poly tetra fluoroethylene (PTFE) mixed in a mass ratio of 5:4:1, and then pasted onto nickel foam (1.0 cm<sup>2</sup>) with catalyst loading of 2.0 mg. The as-fabricated ZAB were characterized using a CHI 760E electrochemical workstation and LAND CT2001A multi-channel battery testing system.

## Results and Discussion

The preparation of ultra small Fe<sub>2</sub>N/N-CNTs was illustrated in Fig. 1. Firstly, FeCl<sub>3</sub>, CNTs and NH<sub>4</sub>HCO<sub>3</sub> were mixed in C<sub>2</sub>H<sub>5</sub>OH

and stirred at room temperature to synthesize FeOOH/CNTs precursors. Then, Fe<sub>2</sub>N/N-CNTs hybrid materials were prepared by calcining FeOOH/CNTs in NH<sub>3</sub> atmosphere. The as-prepared catalysts were investigated by scanning electron microscope (SEM). Compared to SEM images of pure CNTs, FeOOH/CNTs and pure Fe<sub>2</sub>N NPs, there is no obvious change from the SEM image of Fe<sub>2</sub>N/N-CNTs, which may be caused by the small diameter of the Fe<sub>2</sub>N NPs in Fe<sub>2</sub>N/N-CNTs. It indicated that the exist of CNTs can reduce diameter and aggregation of Fe<sub>2</sub>N NPs. The EDS mapping images of Fe, N and C for Fe<sub>2</sub>N/N-CNTs clearly showed that the Fe<sub>2</sub>N was dispersed uniformly on CNTs (Fig. 1f). The crystal structures of the as-prepared samples were studied by X-ray diffraction (XRD). As displayed in Fig. 2a, only two broad peaks were found for pure CNTs. On the other hand, typical diffraction peaks located at around 37.6°, 40.8°, 43.0°, 56.8° and 67.8° were detected, which can be indexed to the (102), (002), (101), (102) and (110) plane of Fe<sub>2</sub>N (JCPDS No. 02-1206). Besides the strong diffraction peaks belong to CNTs, weak diffraction peak at 37.6° were found for Fe<sub>2</sub>N/N-CNTs, suggesting low ratio or weak crystallinity of Fe<sub>2</sub>N in Fe<sub>2</sub>N/N-CNTs hybrid materials.

The X-ray photoemission spectroscopy (XPS) measurement was conducted to analyze the surface chemical composition. Fig. 2b showed C1s core level XPS spectrum of Fe<sub>2</sub>N/N-CNTs, and it can be deconvoluted into four peaks. The peaks at 284.8 eV, 285.1 eV, 288.2 eV and 291.2 eV, were attributed to C-C, C = N, C-O and C = O bonds, respectively.<sup>27-29</sup> Fe 2p XPS core level spectrum of Fe<sub>2</sub>N/N-CNTs in Fig. 2c can be de-convoluted into two valence states, which are ascribed to the reported values for Fe<sup>2+</sup> (724.9 and 710.6 eV) and Fe<sup>3+</sup> (733.2 and 712.2 eV), respectively.<sup>23,30</sup> As shown in Fig. 2d, the N1s XPS spectrum can be deconvoluted into four peaks centered at the binding energy of 403.5 eV, 401.0 eV, 400.1 eV and 398.7 eV, which are correspond with the typical value of oxidized N, graphitic N, Fe-N, and pyridinic N. The functional groups of graphitic N and pyridinic N are considered as highly

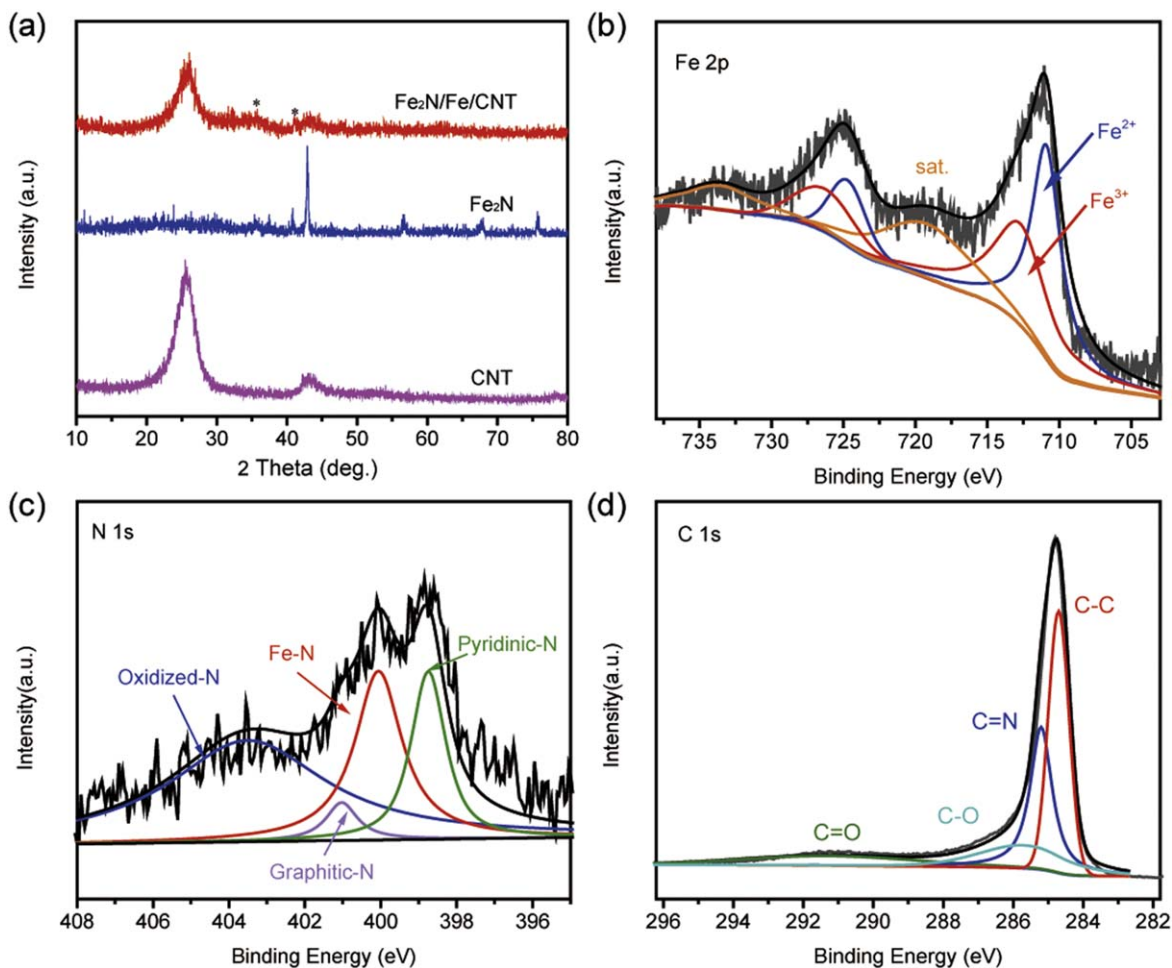


**Figure 2.** (a) XRD patterns of pure CNTs, Fe<sub>2</sub>N NPs and Fe<sub>2</sub>N/N-CNTs. (b) XPS spectra of (a) C 1 s core level, (b) Fe 2p core level and (d) N 1 s core level of Fe<sub>2</sub>N/N-CNTs.

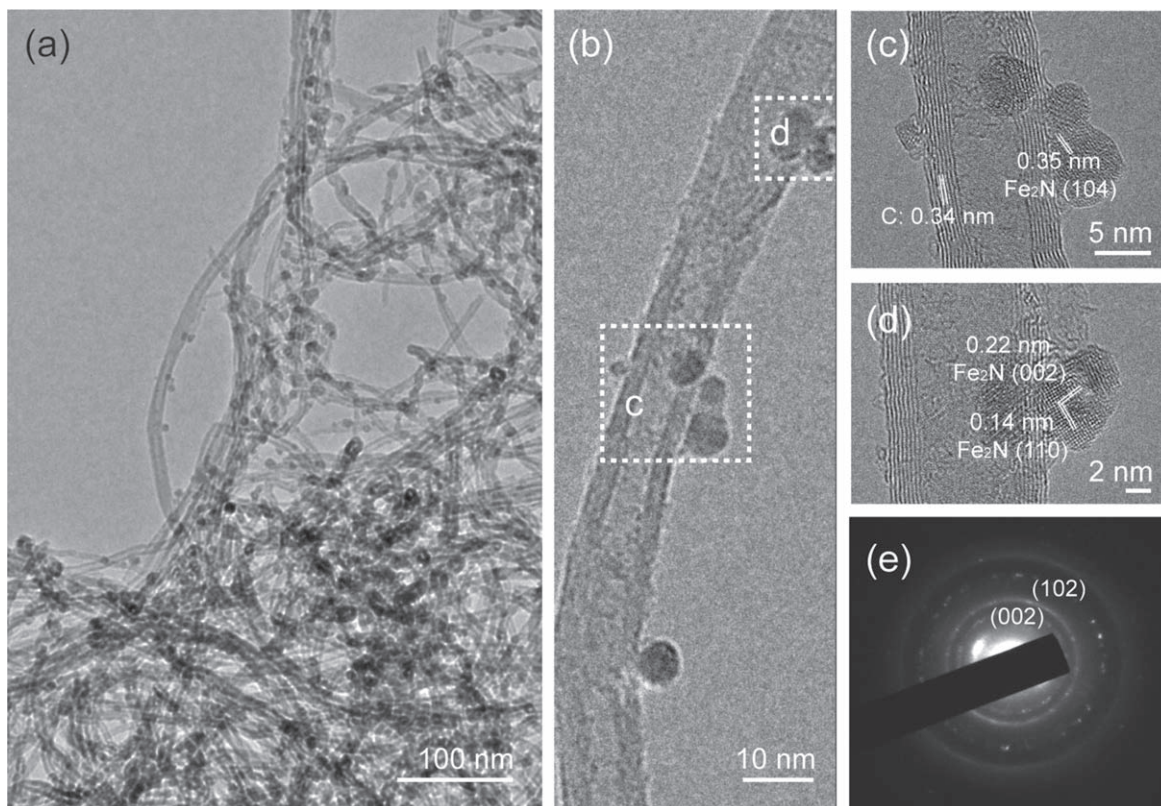
catalytic structures, and lead to improved ORR activity.<sup>31–33</sup> These results confirm the exist of iron nitrides and N doped CNTs.<sup>34,35</sup> The microstructure of Fe<sub>2</sub>N/N-CNTs were further study by transmission electron microscopy (TEM). As shown in Fig 3a, Fe<sub>2</sub>N NPs were well dispersed on the N-CNTs. Typical TEM image of a single CNT was displayed in Fig. 3b, clearly showing the diameter of Fe<sub>2</sub>N NPs are around 5 nm. The HR-TEM images in Figs. 3c–3d showed typical lattice spacing of about 0.35 nm, 0.22 nm and 0.14 nm, corresponding to the (104), (002) and (110) plane of Fe<sub>2</sub>N, respectively. The lattice spacing of about 0.34 nm can be assigned carbon layers. Therefore, the ultra-small Fe<sub>2</sub>N/N-CNTs were successfully synthesized.

In order to evaluate the ORR performance of Fe<sub>2</sub>N/N-CNTs, linear sweep voltammogram (LSV) curves were collected on a rotating disc electrode (RDE) in an O<sub>2</sub>-saturated 0.1 M KOH solution at a scan rate of 10 mV s<sup>-1</sup>. The ORR performance of catalysts was summarized in Fig. 4. The onset potential of Pt/C was 0.95 V vs RHE, which was agreed with recent literatures.<sup>36,37</sup> The onset potential of Fe<sub>2</sub>N was around 0.61 V vs RHE, because of agglomeration of the NPs during the synthesized process. It suggested that electron transport and gas diffusion capabilities of Fe<sub>2</sub>N were limited.<sup>38</sup> Due to the good electrical conductivity, large pore volume and specific surface area of CNTs,<sup>39,40</sup> the ORR activity of Fe<sub>2</sub>N/N-CNTs were significantly improved, with the onset potential of 0.86 V vs RHE. These results indicated that N-CNTs can reduce the diameter and agglomeration of the NPs,<sup>26–40</sup> and it has been confirmed by the SEM and TEM images. Moreover, the half-wave potential of Fe<sub>2</sub>N/N-CNTs was 0.71 V vs RHE, which

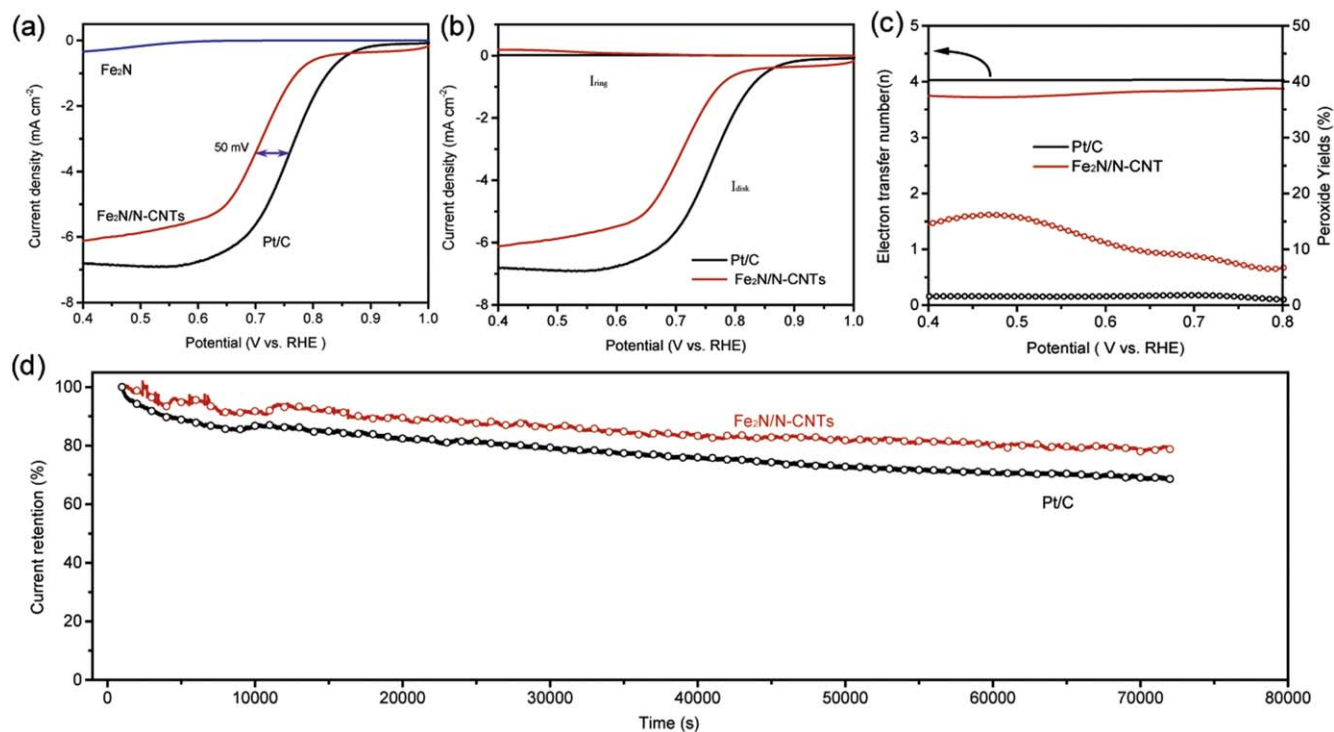
is only 50 mV lower than that of Pt/C (0.76 V vs RHE). It meant that Fe<sub>2</sub>N/N-CNTs electrocatalyst was probably promising candidate for metal-air batteries.

LSV curves on rotating ring-disk electrode (RRDE) electrode were carried out to determine electron transfer number (n) and the H<sub>2</sub>O<sub>2</sub> percent yield (%) of samples during the process of oxygen reduction (Fig. 4c).<sup>19,41</sup> At the range of 0.50 V–0.80 V vs RHE, the average n and H<sub>2</sub>O<sub>2</sub> yield percent was about 3.8 and 7.4% for Fe<sub>2</sub>N/N-CNTs, 4.0 and 1.5% for Pt/C, respectively. These results revealed that Fe<sub>2</sub>N/N-CNTs possessed an apparent quasi-four-electron process. Additionally, the durability is another important issue that should be considered for the design of highly efficient air cathodes. Fig. 4d showed the chronoamperometric responses of both Pt/C and Fe<sub>2</sub>N/N-CNTs tested at a constant voltage of their half-wave potentials. In general, the reduction current density of Fe<sub>2</sub>N/N-CNTs only decrease around 16% of the initial current density, whereas Pt/C showed more than 20% decrease in its initial current density after the same test. It revealed Fe<sub>2</sub>N/N-CNTs possessed excellent durability compared with Pt/C. The XPS spectra of C 1 s, Fe 2p and N 1 s core levels of Fe<sub>2</sub>N/N-CNTs were also collected. As shown in Fig. 5, the iron nitrides and N doped CNTs almost remained unchanged, except that the signals weakened due to the exist of Nafion.

The potential difference or reversible oxygen overpotential of both Fe<sub>2</sub>N/N-CNTs and Pt/C between ORR and OER in 0.1 M KOH is determined to evaluate the bifunctional catalytic activities by following formula:  $\Delta E = E_{j=10} - E_{1/2}$ , where  $E_{j=10}$  was the potential of air cathode to reach the current density of 10 mA cm<sup>-2</sup> for OER.



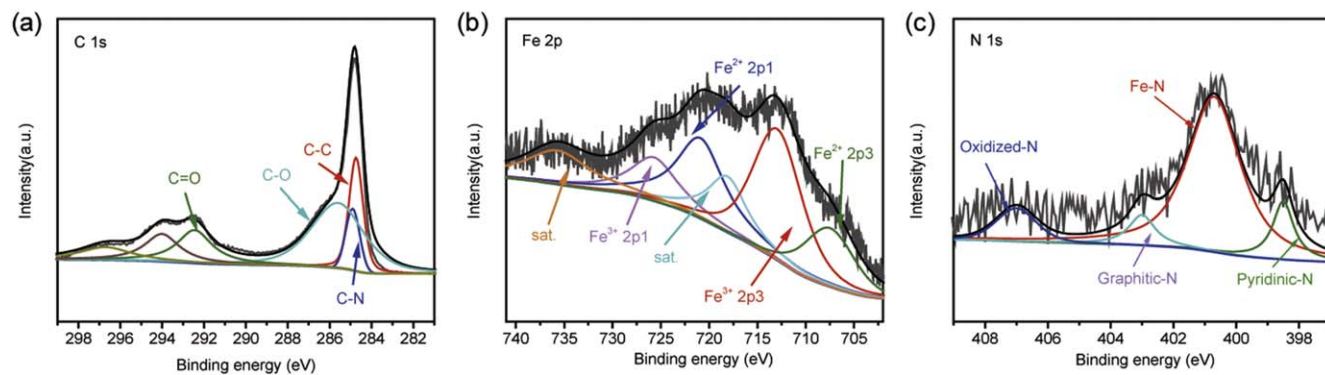
**Figure 3.** (a) TEM images, (b)–(d) HR-TEM images and (e) SEAD image of Fe<sub>2</sub>N/N-CNTs.



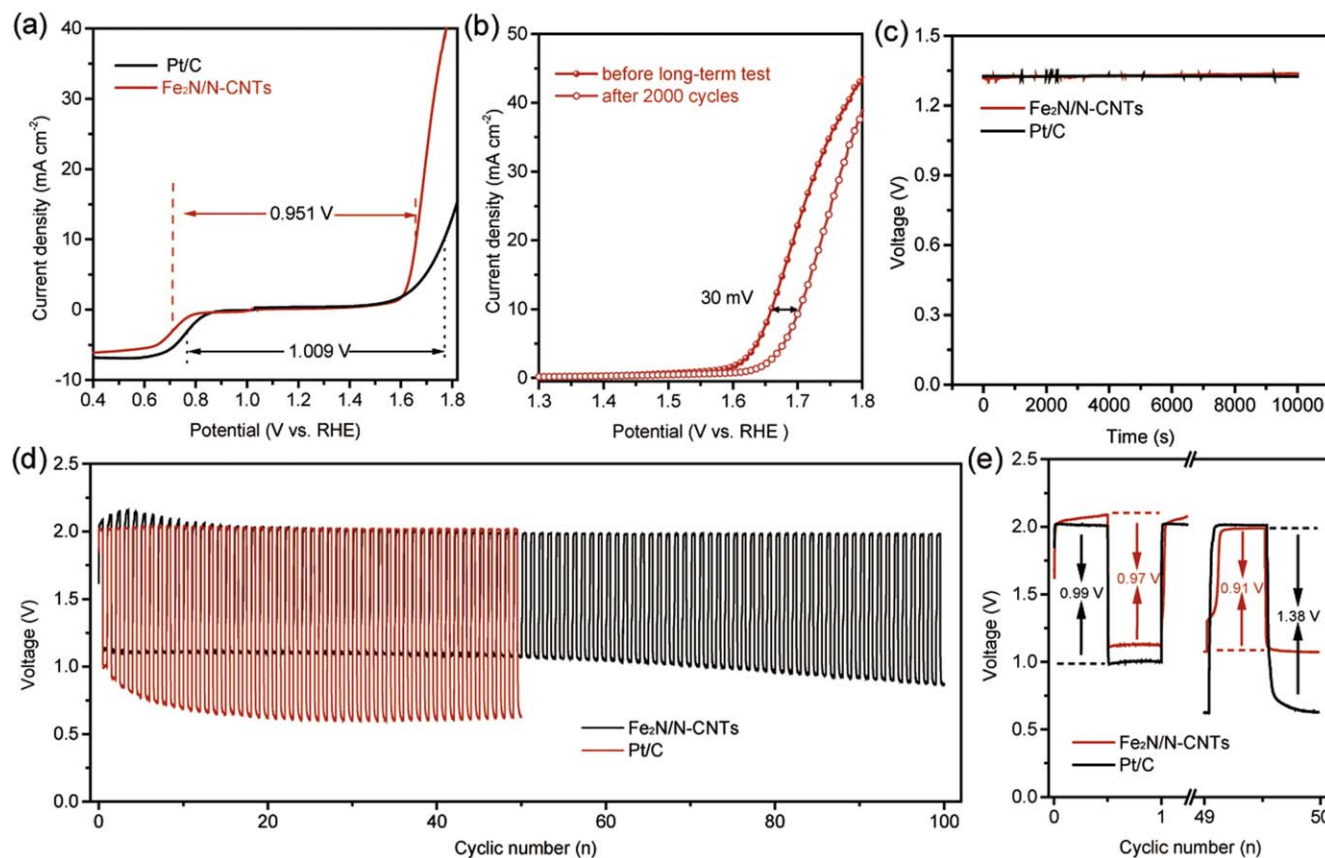
**Figure 4.** (a) RDE and (b) RRDE LSV curves for Fe<sub>2</sub>N, Fe<sub>2</sub>N/N-CNTs and Pt/C in O<sub>2</sub>-saturated 0.1 M KOH at a rotating speed of 1600 rpm. (c) Electron transfer number and peroxide yields of Fe<sub>2</sub>N/N-CNTs and Pt/C calculated from RRDE LSV curves. (d) Chronoamperometric response of Fe<sub>2</sub>N/N-CNTs and Pt/C measured at their half-wave potential with the counter electrode of carbon electrode.

Figure 6a showed that the Fe<sub>2</sub>N/N-CNTs have much smaller reversible oxygen overpotential of around 0.95 V, compared to that of Pt/C (1.01 V). This value was comparable to most recent

literatures, such as N, S-carbon nanosheet (0.88 V),<sup>37</sup> CoO<sub>x</sub>S<sub>1.097</sub>/G (0.96 V),<sup>42</sup> CaMn<sub>4</sub>O<sub>x</sub> (1.04 V).<sup>36</sup> Moreover, the OER stability of the Fe<sub>2</sub>N/N-CNTs electrode was shown in Fig. 6b. It is obvious that the



**Figure 5.** XPS spectra of (a) C 1s core level, (b) Fe 2p core level and (c) N 1s core level of  $\text{Fe}_2\text{N}/\text{N-CNTs}$  after long-term measurement.



**Figure 6.** (a) Bifunctional activities for of  $\text{Fe}_2\text{N}/\text{N-CNTs}$  and Pt/C in 0.1 M KOH solution at 1600 rpm; (b) LSV curves of the  $\text{Fe}_2\text{N}/\text{N-CNTs}$  electrode before and after 2000 cycles; (c) open circuit voltage and (d) cycling stability test of ZABs with  $\text{Fe}_2\text{N}/\text{N-CNTs}$  and Pt/C cathodes; (e) voltage gap of ZABs of  $\text{Fe}_2\text{N}/\text{N-CNTs}$  and Pt/C at the 1st and 49th cycles.

$\text{Fe}_2\text{N}/\text{N-CNTs}$  possessed acceptable durability, which only showed positive shift of around 30 mV after 2000 cycles in 0.1 M KOH.

Encouraged by thus small reversible oxygen overpotential of  $\text{Fe}_2\text{N}/\text{N-CNTs}$ , home-made ZABs were assembled with Zn foil as anode and a mixture solution of 6 M KOH and 0.2 M  $\text{Zn}(\text{CH}_3\text{COO})_2$  as electrolyte. As shown in Fig. 6c, the open circuit voltage ( $V_{\text{oc}}$ ) of ZAB with  $\text{Fe}_2\text{N}/\text{N-CNTs}$  cathode was about 1.35 V. The cycling stability of assembled ZABs was also evaluated by applying galvanostatic charge and discharge current densities of 10  $\text{mA cm}^{-2}$  (Fig. 5c). Initially, the ZABs with  $\text{Fe}_2\text{N}/\text{N-CNTs}$  as air-electrode exhibited charging voltage of 2.1 V and discharging voltage of 1.1 V (Fig. 6d). The voltage gap between the discharge/charge voltage was 0.97 V, similar to that of Pt/C (0.99 V). At the 49th cycle, the voltage gap of  $\text{Fe}_2\text{N}/\text{N-CNTs}$  was nearly (0.91 V) same to the 1st cycle, while the Pt/C increased dramatically to

1.38 V, as shown in Fig. 6e. This result confirmed that the  $\text{Fe}_2\text{N}/\text{N-CNTs}$  had excellent recharge ability. However, it should be pointed out that voltage gap shifted from the initial  $\sim 0.97$  V to 1.10 V at the 60th cycle and 1.15 V at the 100th cycle (ca. 80 h test), which meant there remains substantial room for improvement of bifunctional electrocatalysts.

## Conclusions

In summary, we developed a facile method to prepare ultra-small  $\text{Fe}_2\text{N}/\text{N-CNTs}$  hybrid materials as bifunctional electrocatalysts for ZABs. Due to the ultra-small  $\text{Fe}_2\text{N}$  NPs ( $\sim 5$  nm) and large surface areas of CNTs,  $\text{Fe}_2\text{N}/\text{N-CNTs}$  showed outstanding and efficient activity and durability for ORR and OER. The half wave potential of  $\text{Fe}_2\text{N}/\text{N-CNTs}$  catalysts was about 0.71 V vs RHE, which is

comparable to those of the commercial Pt/C catalysts. In addition, it only possessed outstanding OER activity. Especially, the Fe<sub>2</sub>N/N-CNTs catalysts can be successfully employed as Zn-air batteries, displaying the higher power density and excellent charge-discharging stability than Pt/C electrode. It provides an environmentally friendly and simple method for the preparation of bifunctional electrocatalysts for reversible energy devices.

### Acknowledgments

This work was supported by National Natural Science Foundation of China (No. 21775022, 21703034, 51878169), the Guangdong Innovation Team Project for Colleges and Universities (2016KCXTD023) and Natural Science Foundation of Guangdong Province (No. 2017A030310603).

### References

- J. Pan, Y. Y. Xu, H. Yang, Z. Dong, H. Liu, and B. Y. Xia, *Adv. Sci.*, **5**, 1700691 (2018).
- R. Wang, Z. Chen, N. Hu, C. Xu, Z. Shen, and J. Liu, *Chem. Electro. Chem.*, **5**, 1745 (2018).
- X. Xia, S. Deng, S. Feng, J. Wu, and J. Tu, *J. Mater. Chem. A*, **5**, 21134 (2017).
- Z. Yao, X. Xia, D. Xie, Y. Wang, C. A. Zhou, S. Liu, S. Deng, X. Wang, and J. Tu, *Adv. Funct. Mater.*, **28**, 1802756 (2018).
- Y. Li, G. Cheng, Z. Zhou, X. Liao, S. Han, F. Ye, M. Sun, and L. Yu, *Chem. Electro. Chem.*, **6**, 4429 (2019).
- P. Wang, D. Chen, J. Pan, X. Zeng, Y. Sun, Y. Lin, X. Shu, and X. Jin, *J. Electrochem. Soc.*, **166**, A968 (2019).
- H. Han, S. Chao, Z. Bai, X. Wang, X. Yang, J. Qiao, Z. Chen, and L. Yang, *Chem. Electro. Chem.*, **5**, 1868 (2018).
- S. Guo, S. Zhang, and S. Sun, *Angew. Chem. Int. Ed.*, **52**, 8526 (2013).
- L. Jørisen, *J. Power Sources*, **155**, 23 (2006).
- R. K. Bera, H. Park, and R. Ryoo, *J. Mater. Chem. A*, **7**, 9988 (2019).
- J. He, C. Wu, L. Song, L. Li, W. Xia, C. Jiang, B. Gao, Y. Du, and T. Wang, *Chem. Electro. Chem.*, **6**, 4010 (2019).
- F. L. Meng, K. H. Liu, Y. Zhang, M. M. Shi, X. B. Zhang, J. M. Yan, and Q. Jiang, *Small*, **14**, e1703843 (2018).
- Y. Xie, Y. Yang, Q. Zhou, L. Wang, Y. Yao, X. Zhu, L. Fang, H. Zhao, and J. Zhang, *J. Electrochem. Soc.*, **166**, H549 (2019).
- R. A. Senthil, J. Pan, X. Yang, and Y. Sun, *Int. J. Hydrogen Energy*, **43**, 21824 (2018).
- E. Farjami and L. J. Deiner, *J. Electrochem. Soc.*, **162**, H571 (2015).
- Y. Zhang et al., *Chem. Mater.*, **30**, 4762 (2018).
- D. Zhou et al., *Adv. Energy Mater.*, **8**, 1701905 (2018).
- C. Guan, A. Sumboja, W. Zang, Y. Qian, H. Zhang, X. Liu, Z. Liu, D. Zhao, S. J. Pennycook, and J. Wang, *Energy Storage Mater.*, **16**, 243 (2019).
- L. Chen, Y. Zhang, X. Liu, L. Long, S. Wang, X. Xu, M. Liu, W. Yang, and J. Jia, *Carbon*, **151**, 10 (2019).
- R. A. Senthil, Y. Wang, S. Osman, J. Pan, Y. Lin, X. Shu, X. Jin, and Y. Sun, *Int. J. Hydrogen Energy*, **44**, 16537 (2019).
- X. Wang, F. Zhang, Y. Liu, and Z. Wang, *J. Electrochem. Soc.*, **165**, J3052 (2018).
- A. Sumboja, M. Lübke, Y. Wang, T. An, Y. Zong, and Z. Liu, *Adv. Energy Mater.*, **7**, 1700927 (2017).
- X. Huang, Z. Yang, B. Dong, Y. Wang, T. Tang, and Y. Hou, *Nanoscale*, **9**, 8102 (2017).
- Z. Qiao, H. Zhang, S. Karakalos, S. Hwang, J. Xue, M. Chen, D. Su, and G. Wu, *Appl. Catal. B: Environ.*, **219**, 629 (2017).
- J. Xiao, Y. Xu, Y. Xia, J. Xi, and S. Wang, *Nano Energy*, **24**, 121 (2016).
- J. Liu, M. Zheng, X. Shi, H. Zeng, and H. Xia, *Adv. Funct. Mater.*, **26**, 919 (2016).
- Y. Zhong, X. Xia, S. Deng, D. Xie, S. Shen, K. Zhang, W. Guo, X. Wang, and J. Tu, *Adv. Mater.*, **30**, 1805165 (2018).
- S. Shen, X. Xia, Y. Zhong, S. Deng, D. Xie, B. Liu, Y. Zhang, G. Pan, X. Wang, and J. Tu, *Adv. Mater.*, **31**, 1900009 (2019).
- X. Xia, S. Deng, D. Xie, Y. Wang, S. Feng, J. Wu, and J. Tu, *J. Mater. Chem. A*, **6**, 15546 (2018).
- Z.-Y. Chen, Y.-N. Li, L.-L. Lei, S.-J. Bao, M.-Q. Wang, H.-L. Heng-Liu, Z.-L. Zhao, and M.-W. Xu, *Catal. Sci. Technol.*, **7**, 5670 (2017).
- R. Akram, M. A. Ud Din, S. U. Dar, A. Arshad, W. Liu, Z. Wu, and D. Wu, *Nanoscale*, **10**, 5658 (2018).
- Z. Liu, J. Liu, H. B. Wu, G. Shen, Z. Le, G. Chen, and Y. Lu, *Nanoscale*, **10**, 16996 (2018).
- S. Han, X. Hu, J. Wang, X. Fang, and Y. Zhu, *Adv. Energy Mater.*, **8**, 1800955 (2018).
- Y. Qiao, P. Yuan, Y. Hu, J. Zhang, S. Mu, J. Zhou, H. Li, H. Xia, J. He, and Q. Xu, *Adv. Mater.*, **30**, e1804504 (2018).
- X. Liu, L. Wang, P. Yu, C. Tian, F. Sun, J. Ma, W. Li, and H. Fu, *Angew. Chem. Int. Ed.*, **57**, 16166 (2018).
- Y. Gorlin and T. F. Jaramillo, *J. Am. Chem. Soc.*, **132**, 13612 (2010).
- K. Qu, Y. Zheng, S. Dai, and S. Z. Qiao, *Nano Energy*, **19**, 373 (2016).
- Z. W. Seh, J. Kibsgaard, C. F. Dickens, I. Chorkendorff, J. K. Nørskov, and T. F. Jaramillo, *Science*, **355** (2017).
- X. Chen, Z. Zhou, H. E. Karahan, Q. Shao, L. Wei, and Y. Chen, *Small*, **14**, e1801929 (2018).
- F. Xu, L. Chang, X. Duan, W. Bai, X. Sui, and X. Zhao, *Electrochim. Acta*, **300**, 53 (2019).
- J. Wu et al., *Appl. Catal. B: Environ.*, **254**, 55 (2019).
- J. Fu, F. M. Hassan, C. Zhong, J. Lu, H. Liu, A. Yu, and Z. Chen, *Adv. Mater.*, **29**, 1702526 (2017).